ICNTS - Benchmarking of Momentum Correction Techniques

Craig D. BEIDLER[1)], Maxim Yu. ISAEV[2)], Sergei V. KASILOV[3,4)], Winfried KERNBICHLER[4)], Georg O. LEITOLD[4)] Henning MAASSBERG[1)], Sadayoshi MURAKAMI[5)], Victor V. NEMOV[3,4)], Donald A. SPONG[6)], Victor TRIBALDOS[7)]

[1)] *Max-Planck Institut für Plasmaphysik, Association EURATOM, Greifswald, Germany*
[2)] *Russian Research Center "Kurchatov Institute", Moscow, Russia*
[3)] *Insitute of Plasma Physics, NSC-KhIPT, Kharkov, Ukraine*
[4)] *Insitut für Theoretische Physik, Association EURATOM-ÖAW, TU-Graz, Austria*
[5)] *Department of Nuclear Engineering, Kyoto University, Kyoto, Japan*
[6)] *Oak Ridge National Laboratory, Oak Ridge, Tennesee, USA*
[7)] *Laboratorio Nacional de Fusión, CIEMAT, Association EURATOM, Madrid, Spain*

October 11, 2007

In the traditional neoclassical ordering, mono-energetic transport coefficients are evaluated using the simplified Lorentz form of the pitch-angle collision operator which violates momentum conservation. In this paper, the parallel momentum balance with radial parallel momentum transport and viscosity terms is analysed, in particular with respect to the radial electric field. Next, the impact of momentum conservation in the stellarator *lmfp*-regime is estimated for the radial transport and the parallel electric conductivity. Finally, momentum correction techniques are described based on mono-energetic transport coefficients calulated e.g. by the DKES code, and preliminary results for the parallel electric conductivity and the bootstrap current are presented.

Keywords: ICNTS, neoclassical transport, stellarators, parallel momentum conservation

1. Introduction

The *International Collaboration on Neoclassical Transport in Stellarators* (ICNTS) was initiated in 2000. The starting point is the drift-kinetic equation (DKE) which is linearised with respect to the *1st-order* distribution function defined as the (small) deviation from the *0th-order* (unshifted) Maxwellian, F_M, with the density, electrostatic potential and temperature assumed to be constant on flux-surfaces. The *1st-order* DKE becomes inhomogeneous with a radial driving force, $-\dot{r}\, F_M'$ ($\dot{r}$ being the radial component of the ∇B-drift velocity and F_M' the radial derivative of the Maxwellian with total energy conserved), and with a parallel driving force, $\propto v_\| \, B \, F_M$. Splitting this DKE with respect to the driving forces leads to two *1st-order* distribution functions, f and g, where f is related to $-\dot{r}\, F_M'$ (symmetric in $v_\|$) and g to $v_\| \, B \, F_M$. The Vlasov operator couples symmetric and asymmetric terms; consequently, f (g) has also asymmetric (symmetric) contributions. With the linearised collision operator, $C^{\rm lin}$, the parallel momentum balances are given by

$$\frac{1}{V'}\frac{d}{dr}V'\left[\!\!\left[B\dot{r}v_\| \, {f \atop g} \right]\!\!\right] - \left[\!\!\left[\frac{\mathbf{B}\cdot\boldsymbol{\nabla}B}{B}\,(v_\|^2-\frac{1}{2}v_\perp^2)\,{f \atop g} \right]\!\!\right] - \left[\!\!\left[\frac{\mathbf{B}\times\boldsymbol{\nabla}\Phi}{\langle B^2\rangle}\cdot\boldsymbol{\nabla}B\,v_\|\,{f \atop g} \right]\!\!\right] - \left[\!\!\left[Bv_\| C^{\rm lin}\begin{pmatrix} f \\ g \end{pmatrix} \right]\!\!\right] = {0 \atop \frac{1}{2}v_{th}^2\langle B^2\rangle} \qquad (1)$$

where $[\![...]\!]$ means flux-surface averaging and velocity space integration and Φ the electrostatic potential. Here, the incompressible form of the $\mathbf{E}\times\mathbf{B}$ drift is used for consistency with e.g. DKES (Drift-Kinetic Equation Solver) [1, 2] and both momentum correction techniques [3, 4] described later. The important advantage of this approximation is the disappearance of the $(\mathbf{B}\times\boldsymbol{\nabla}\Phi)\cdot\boldsymbol{\nabla}B$ term in both acceleration terms, $\dot{p}$ and $\dot{v}$ ($p = v_\|/v$), in the conservative formulation; see [5]. Then, $\dot{p} \propto \mathbf{B}\cdot\boldsymbol{\nabla}B$, i.e. the mirror term, and $\dot{v} = 0$ allowing for a mono-energetic treatment of the *1st-order* DKE if the collision operator is replaced by the simple Lorentz form of the pitch-angle collision term which, however, violates momentum conservation. As shown in [5], the incompressibility approximation in the *1st-order* DKE is justified for radial electric fields, E_r, nearly up to the toroidal resonance value, $E_r^{\rm res} = \iota\epsilon vB$.

The 1st term in the parallel momentum balances (1) describes the radial transport of parallel momentum which, in general, is ignored in the traditional neoclassical theory (see e.g. the review [6]). In an axisymmetric configuration with $E_r = 0$, the $sin\theta$ part of f (symmetric in p) leads to the particle transport whereas the $cos\theta$ part (asymmetric in p) finally leads to the bootstrap current coefficient. This separation is broken at larger E_r: the $sin\theta$ component of f has also asymmetric contributions leading to radial transport of parallel momentum. The parallel momentum transport coefficients in mono-energetic form equivalent to eq.(1) are calculated with a new DKES ver-

author's e-mail: Henning.Maassberg@ipp.mpg.de

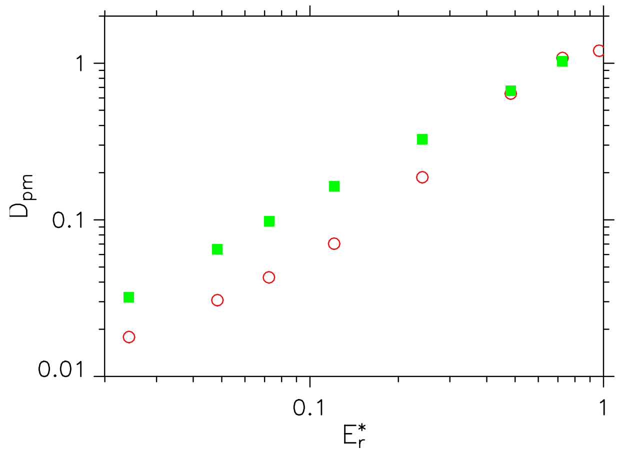

Fig. 1 Mono-energetic parallel momentum transport coefficients, D_{p1}/D_{11} (open circle) and D_{p3}/D_{13} (full square), vs. the normalised radial electric field, E_r^* for the LHD-360 configuration at $\nu^* = 7.2 \cdot 10^{-5}$.

sion. In Fig. 1, the mono-energetic $D_{p1} = [\dot{r}pf]$ (normalised to the particle transport coefficient $D_{11} = [\dot{r}f]$) and $D_{p3} = [\dot{r}pg]$ (normalised to the Ware pinch coefficient $D_{13} = [\dot{r}g] = -D_{31} = -[pf]$) are shown for rather large E_r (normalised to the toroidal resonance value, $E_r^* = E_r/E_r^{\mathrm{res}}$, for the LHD vacuum configuration with $R = 3.60$ m at half the plasma radius. (Here, [...] means integration over p and flux-surface averaging.) The value of the collisionality, $\nu^* = \nu R/\iota v$, places these results in the *lmfp*-regime. For an axisymmetric configuration where both D_{11} and D_{13} are independent of E_r (for $E_r^* \ll 1$), D_{p1}/D_{11} slightly exceeds D_{p3}/D_{13}, and both terms scale linearly in E_r^*. These results lead to a strong restriction for the radial electric field: only for $E_r^* \ll 1$, does the radial transport of parallel momentum become negligible. This restriction is stronger than the one related to validity of the incompressible $\mathbf{E} \times \mathbf{B}$ approximation; see [5]. Furthermore, also the 3rd term in eq.(1), the viscosity related to the $\mathbf{E} \times \mathbf{B}$ flow, can be ignored for $E_r^* \ll 1$.

The 2nd term in the parallel momentum balances (1) is the parallel viscosity describing the damping of parallel flows due to the magnetic field inhomogenity. In an asymptotic collisionless limit, the *1st-order* DKE for g (parallel driving force) can be directly integrated for sufficiently small E_r following Refs. [7, 8]. By flux-surface averaging, the 1st Legendre component of the DKE reduces to a 1D equation for the velocity dependence of the asymmetric part of g (here only for ions)

$$g^a = -\frac{\langle b^2\rangle}{2\nu_{ii}(x)}\,\frac{1}{f_c}\,K(x)\int_0^1 \frac{\lambda\,d\lambda}{\langle\sqrt{1-\lambda b}\rangle}$$

and

$$C_{ii}^1(K) - \frac{f_t}{f_c}\,\nu_{ii}(x)\,K = \nu_{i0}xF_M,$$

with the thermal ion collision frequency, ν_{i0}, $x = v/v_{th}$, $b = B/B_{\max}$, and with the trapped particle fraction

$$f_t = 1 - f_c = 1 - \frac{3}{4}\langle b^2\rangle \int_0^1 \frac{\lambda\,d\lambda}{\langle\sqrt{1-\lambda b}\rangle}.$$

$g^a(\lambda > 1) = 0$ for trapped particles. C_{ii}^1 is the 1st Legendre component of C^{lin}, ion-electron collisions can be neglected. Impurities can act as an additional momentum sink (but are ignored here for simplicity). In this collisionless picture, the viscous damping of the parallel ion flow is equivalent to the friction of the passing with the trapped ions. In an equivalent approach [9], the collisionless electric conductivity is obtained.

2. Simple Pictures of Momentum Corrections

The computations of even mono-energetic transport coefficients (e.g. by DKES) are rather time expensive in the *lmfp*-regime. The treatment of the linearised collision operator with momentum conservation would require the solution of the DKE in the 4D-phase space instead of the 3D mono-energetic solution. Consequently, momentum correction techniques [3, 4] based on the mono-energetic transport coefficients become attractive. A rough estimation of the correction, however, can be obtained from eq.(1) with incompressible $E \times B$ flow for the different transport coefficients. The *1st-order* distribution functions are split: $f = f_1 + f_2$ and $g = g_1 + g_2$ where f_1 and g_1 are the solutions of the mono-energetic DKE with the Lorentz form of the pitch angle collision term, C^p, instead of C^{lin}. Then, the corrections f_2 and g_2 are defined by

$$V\begin{pmatrix} f_2 \\ g_2\end{pmatrix} - C^{\mathrm{lin}}\begin{pmatrix} f_2 \\ g_2\end{pmatrix} = C^{\mathrm{lin}}\begin{pmatrix} f_1 \\ g_1\end{pmatrix} - C^{p}\begin{pmatrix} f_1 \\ g_1\end{pmatrix}$$

Neglecting parallel momentum transport and the $\mathbf{E} \times \mathbf{B}$-viscosity term for sufficiently small E_r leads to the balance equations for the 1st and 2nd Legendre components of the corrections, f_2 and g_2,

$$\left[\mathbf{B}\cdot\boldsymbol{\nabla}B\,P_2(p)\,\frac{f_2}{g_2}\right] + \frac{3}{2}\,C^{\mathrm{lin}}\left(\left[B\,p\frac{f_2}{g_2}\right]\right) = \nu\,\frac{D_{31}}{D_{33}} - C^{\mathrm{lin}}\begin{pmatrix} D_{31} \\ D_{33}\end{pmatrix} \quad (2)$$

where $D_{31}(v) = [pf_1]$ and $D_{33}(v) = [pg_1]$ are the mono-energetic transport coefficients, calculated e.g. by DKES, and $P_2(p)$ is the 2nd Legendre polynomial.

In the *lmfp*-regime, the parallel viscosity evaluated for f_1 (by DKES) is proportional to $\nu*$, and only weakly dependent on E_r. Although this term is also determined by the symmetric component of f_1, the large $D_{11} = [\dot{r}f_1]$ has a quite different dependence on ν^* and E_r, e.g. in the $1/\nu$- and the $\sqrt{\nu}$-regimes. If any distribution function is split into a slow and a fast scale with respect to bounce-averaging, the slow part determines D_{11} [10], but does not contribute to the parallel viscosity. This can be shown by formulating the flux-surface averaging as bounce-averaging for the ripple-trapped particles, and the slow contribution vanishes due to the $\mathbf{B}\cdot\nabla B$ term (different to $\mathbf{B}\times\nabla B$ in $\dot{r}$). Consequently, the impact of momentum conservation on the radial transport in the stellarator *lmfp*-regime is negligible. For tokamaks, however, the situation is different. Here, the radial transport coefficients in the *lmfp*-regime (banana regime) are proportional to ν^* and corrections from the momentum conservation are not negligible. NEO-2 [11], based on the field-line integration technique, is generalised for a full linearised collision operator with momentum conservation. As shown in Ref. [12], the radial transport coefficients are reduced whereas the bootstrap current coefficient are increased with the full linearised collision operator compared to the Lorentz model.

The impact of momentum conservation for the parallel electric conductivity is of the order of 100%. The classical "Spitzer problem" in the collisional limit [13] can be analytically generalised to the collisionless limit [9]. The collisionless Spitzer function, $K(x)$, is defined by the 1D integro-differential equation in $x = v/v_{th}$

$$C_{ee}^1(K) - \left(\frac{f_t}{f_c}\,\nu_{ee}(x) + \frac{\nu_{e0}}{x^3}Z_{\rm eff}\right)K = \nu_{e0}xF_M,$$

with the thermal electron-ion collision frequency, ν_{e0}, and the (energy-dependent) electron-electron collision frequency, $\nu_{ee}(x)$. C_{ee}^1 is the 1st Legendre moment of the linearised collision operator. The classical "Spitzer problem" corresponds to $f_t = 0$. In the mono-energetic approach, the normalised $D_{33}/\nu^* = 1$ in the collisional limit and is reduced to the passing (circulating) particle fraction, $D_{33}/\nu^* = f_c$, i.e. the trapped particles defined by f_t do not contribute. With momentum conservation, a stronger weighting of the trapped particles appears (defined by f_t/f_c) which reflects the passing-trapped electron fricton adding to the friction with ions and impurities (defined by the $Z_{\rm eff}$ term). Rather accurate approximations of both the collisional and collisionless Spitzer function, $K(x)$, have been developped; see [14] and [9], respectively. Momentum correction is important for the parallel electric conductivity for all collisionalities.

Fig. 2 shows the benchmarking for the parallel electric conductivity, σ^*, normalised to the collisional Spitzer-Härm value [6] for the W7-X high-mirror (*w7x-hm1*) and low-mirror (*w7x-lm1*) vacuum configurations at $r_a \simeq 1$ with $f_t = 0.5454$ and $f_t = 0.3536$, respectively. Instead of the Maxwellian, the collisional Spitzer function is used in the energy convolution of the mono-energetic DKES coefficients, D_{33} (solid lines). This approach was already used for the evaluation of the experimental current balance in W7-AS; see e.g. [15]. The first preliminary results (full circles) of the momentum correction technique developed by Taguchi [3] agree quite well with the simplified (collisional) correction technique implemented in the DKES energy convolution. (These data are normalised to the DKES data at the highest ν^*, so far). Furthermore, the asymptotic

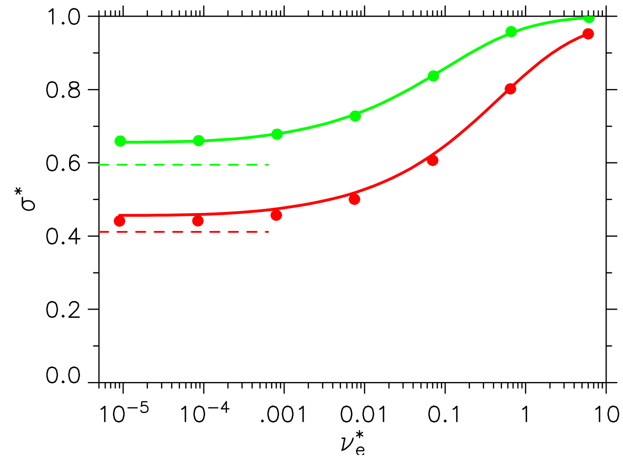

Fig. 2 Parallel electric conductivity, σ^*, normalised to the collisional Spitzer-Härm value vs. the electron collisionality for the high- and low-mirror W7-X configurations (lower and upper curves, respectively) at half the plasma radius for $Z_{\rm eff} = 1$. σ^* based on the collisionless Spitzer function is given for reference (dashed lines).

limit $\nu^* \rightarrow 0$ based on the collisionless Spitzer function with all the trapped-particle effects included (completely kinetic modelling) is given for reference (dashed lines).

3. Momentum Correction Techniques

The momentum correction techniques [3, 4] are based on moment methods, i.e. a low-order expansion of the kinetic equation with the linearised collision operator both in Legendre (with respect to p) and in Sonine (with respect to x) polynomials. With flux-surface averaging, a linear system of equations is obtained which can be closed by using the 3 mono-energetic transport coefficients calculated numerically for different collisionalities and radial electric fields. In particular, the parallel particle and heat viscosities defined by the 2nd Legendere coefficients of f_2 and g_2 in eq.(2) are obtained. The expansion of the linearised collision operator couples the radial transport and parallel flows of all species, and, consequently, the *thermodynamic fluxes* are corrected and not the transport coefficients of each species. An exception is the parallel electric conductivity where ion effects can be neglected. As dicussed in the previous section, the radial transport in the stellarator *lmfp*-regime is nearly unaffected by the momentum correction.

Both momentum correction techniques have been implemented in the energy convolution based on databases of the 3 mono-energetic DKES transport coefficients. Results by using the [4] approach are given in [16, 17]. Recently, benchmarking was initiated, however, this activity is only in the preliminary phase (i.e. benchmarking the interfaces to the DKES data and the energy convolution algorithms). Rather preliminary results for the impact of the momentum conservation technique [3] for the bootstrap current density are shown in Fig. 3 both for the W7-X low- and high-mirror configuration (equivalent to Fig. 2). In these

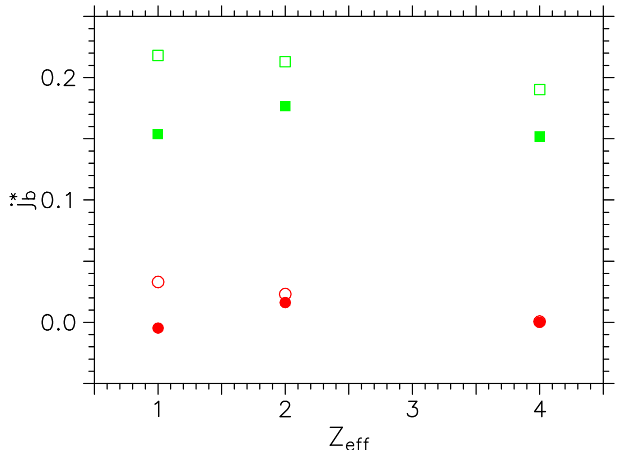

Fig. 3 Bootstrap current density, j_b^* (normalised to the equivalent tokamak value without momentum correction for $E_r = 0$), vs. $Z_{\rm eff}$ without (open symbols) and with momentum correction (full symbols) for the W7-X low-mirror (squares) and for the W7-X high-mirror configuration (circles) at half the plasma radius based on Taguchi's momentum correction technique [3].

calculations, an additional impurity species (fully ionised carbon) was introduced to describe the impact of $Z_{\rm eff}$ on the momentum balance. The radial electric field was calculated from the ambipolarity condition, and, additionally, the impurity density gradient from the condition of vanishing radial impurity flux. The inverse gradient lengths, n'/n and T'/T (with $T_e = T_i = T_C$) are the same for all scenarios. The plasma parameters correspond to low collisionalities, and an "ion-root" E_r is established. Since the electron transport coefficients in the $1/\nu$-regime are reduced with increasing $Z_{\rm eff}$ (and also the bulk ion density), this complex $Z_{\rm eff}$-dependence is eliminated by the normalisation of the bootstrap current density (sum over all species) to the equivalent tokamak value for the same $Z_{\rm eff}$ for $E_r = 0$, but without momentum conservation. With this normalisation, the impact of the momentum conservation on the bootstrap current is highlighted.

Momentum correction has only a moderate impact on the bootstrap current for both W7-X configurations; see Fig. 3. With this correction, the bootstrap current is reduced (a slight increase, however, was found in NEO-2 calculations for a tokamak case with $E_r = 0$). Momentum correction is largest at $Z_{\rm eff} = 1$ and becomes less important at higher $Z_{\rm eff}$, and the optimisation criterion of minimised bootstrap current is not affected which is realised in the W7x high-mirror configuration, at least for small E_r. Furthermore, the radial particle and energy fluxes are nearly identical with and without momentum correction as was analysed in Sec. 2.

Also the NEO-2 version with the momentum conserving collision operator [11] will be included in the benchmarking. NEO-2 expands the distribution function to higher orders in the Sonine polynomials compared to Refs. [3, 4] and solves for the full linearised collision operator. The distribution function is evaluated by the field-line integration technique which leads to the restriction $E_r = 0$. In the strict sence, NEO-2 is not a momentum correction technique since it is not based on the 3 mono-energetic transport coefficients. With the higher accuracy of the expansion, NEO-2 is an attractive tool for benchmarking with both momentum correction techniques described above.

4. Discussion/Conclusions

The benchmarking of momentum correction techniques has been initiated and preliminary results have been obtained. The particle and energy fluxes (and, consequently, the ambipolar radial electric field) in the stellarator *lmpf*-regime are only weakly affected by the violation of momentum conservation in the simplified pitch-angle collision operator used in evaluating the mono-energetic transport coefficients in all codes included in the ICNTS activity. The impact of momentum conservation on estimating the parallel electric conductivity is very well known, and the correction is rather large. Preliminary results for the bootstrap current indicate a moderate reduction with momentum conservation taken into account. Very good agreement is obtained in the benchmarking of mono-energetic bootstrap current coefficients [18]. Consequently, a detailed analysis of momentum conservation effects is a logical next step in the ICNTS.

[1] S.P. Hirshman *et al.*, Phys. Fluids **29**, 2951 (1986).
[2] W.I. van Rij and S.P. Hirshman, Phys. Fluids **B1**, 563 (1989).
[3] M. Taguchi, Phys. Fluids **B4**, 3638 (1992).
[4] H. Sugama and S. Nishimura Phys. Plasmas **9**, 4637 (2002).
[5] C.D. Beidler *et al.*, *ICNTS - Impact of Incompressible $E \times B$ Flow in Estimating Mono-Energetic Transport Coefficients*, this workshop, (2007).
[6] F.L. Hinton and R.D. Hazeltine, Rev. Mod. Physics **48**, 239 (1976).
[7] M. Taguchi, Plasma Phys. Control. Fusion **30**, 1897 (1988).
[8] M. Taguchi, Plasma Phys. Control. Fusion **31**, 241 (1989).
[9] M. Romé *et al.*, Plasma Phys. Control. Fusion **40**, 511 (1998).
[10] A.A. Galeev and R.Z. Sagdeev, Review of Plasma Physics **7**, 307 (1977).
[11] W. Kernbichler *et al.*, *32nd EPS Conf. Plasma Phys., Tarragona 2005*, http://epsppd.epfl.ch/Tarragona/pdf/P1_111.pdf (2005).
[12] W. Kernbichler *et al.*, *33rd EPS Conf. Plasma Phys., Rome 2006*, http://epsppd.epfl.ch/Roma/pdf/P2_189.pdf (2006).
[13] L. Spitzer and R. Härm, Phys. Rev. **89**, 977 (1953).
[14] S.P. Hirshman, Phys. Fluids **23**, 1238 (1980).
[15] H. Maaßberg *et al.*, Plasma Phys. Control. Fusion **47**, 1137 (2005).
[16] D.A. Spong, Phys. Plasmas **12**, 056114 (2005).
[17] D.A. Spong *et al.*, Nucl. Fusion **45**, 918 (2005).
[18] K. Allmaier *et al.*, *ICNTS - Benchmarking of Bootstrap Current Coefficients*, this workshop, (2007).